Georg Lukas Schafhauser, BSc

Automation of a Transmission Line Pulsing Laboratory Setup

MASTER'S THESIS

to achieve the university degree of

Diplom-Ingenieur

Master's degree programme: Telematics

submitted to

Graz University of Technology

Supervisor

Univ.-Prof. Dipl.-Ing. Dr.techn. Bernd Deutschmann

Institute of Electronics

Graz, May 2016

AFFIDAVIT

I declare that I have authored this thesis independently, that I have not used other than the declared sources/resources, and that I have explicitly indicated all material which has been quoted either literally or by content from the sources used. The text document uploaded to TUGRAZonline is identical to the present master‘s thesis dissertation.

Date

Signature

Acknowledgments

First of all, I want to thank my supervisor Prof. Bernd Deutschmann for offering me the opportunity to participate in an exciting research project in a very nice working group.
Furthermore, I want to thank Patrick Schrey for supporting me with his expertise, for encouragements and his patience.

Kurzfassung

Das Phänomen der elektrostatischen Entladung stellt ein zunehmendes Problem für die Elektronikindustrie dar. Elektrostatische Entladungen können zu ernsthaften Beeinträchtigungen von elektronischen Bauteilen führen. Diese Beeinträchtigungen reichen von Parameteränderungen bis zur Zerstörung des Bauteils.
Im Zuge dieser Masterarbeit wurde ein Konzept erstellt, mit dem die Wirkung elektrostatischer Entladung auf elektronische Bauteile automatisiert getestet werden kann. Als Testmethode wird das sogenannte Transmission Line Pulsing verwendet. Die Automatisierung beruht auf einem Gravitations-Testhandler, der die Bauteile automatisiert auf einer Testplatine positioniert.
Darüber hinaus wurde ein Softwarepaket entwickelt, welches die Kontrolle der Messinstrumente übernimmt. Der Test- und Messaufbau wurde dahingehend vorbereitet, Wunsch-Bell Charakteristiken elektronischer Bauteile automatisch zu erstellen.
Die Wunsch-Bell Charakteristiken können dazu verwendet werden, die Robustheit elektronischer Bauteile, gegenüber elektrostatischer Entladungen, abzuschätzen. Dies ermöglicht Elektronikdesignern bessere Schutzstrukturen zu entwerfen.
Schlussendlich wurde in dieser Masterarbeit ein RS-485 Transceiver Chip mit einer unbekannten internen Schutzstruktur untersucht, um die Funktion des Testsetups und der Software zu verifizieren.

Abstract

The electrostatic discharge phenomenon is a major problem in the electronic industry. Electrostatic discharge can lead to serious damages in electronic devices. These damages can range from shifts in parameters to destruction. In the course of this thesis an automated test concept for electrostatic discharge events has been developed. The test approach is Transmission Line Pulse testing. The automation is based on a gravity test handler, which automatically places the devices on a test board.
Furthermore, a software package for controlling the measurement equipment has been designed and implemented. The test and measurement setup has been prepared to generate Wunsch-Bell characteristics of electronic devices automatically.
These Wunsch-Bell characteristics may be used to predict the robustness of electronic devices. This constitutes a huge benefit for electronic designers, because it enables them to develop more reliable protection structures.
Within this thesis a RS-485 transceiver chip with an unknown internal protection structure has been investigated to verify the test setup and software.

Contents

List of Figures

List of Figures

Listings

1 Introduction

1.1 Motivation

Electrostatic discharge (ESD) is a major problem in the electronic industry. Therefore, it is necessary to develop robust and efficient protection structures for electronic devices. For evaluating ESD protection structures a high quality and reliable test procedure is required.

The dominating test procedures today merely provide the information "pass" or "fail". Furthermore, these tests depend on several parameters as the manufacturer of the tester, the contact angle, etc.

The Wunsch-Bell characterization provides a simple means to predict the robustness of electronic devices against arbitrary pulse forms. Transmission Line Pulse (TLP) testing, which stresses the device with a rectangular shaped pulse, is a common method to obtain a Wunsch-Bell characteristic.

Based on Wunsch-Bell characteristics it is possible to obtain simulation models and to predict the robustness of the whole system, given the characterization of the single components, only. To this end, the manufacturers of integrated circuits (ICs) do not have to reveal secret data.

Modern chips can have up to several hundred pins. In a testing procedure all possible pin combinations have to be tested. In order to perform these tests in a reasonable time, an automated testing procedure is required. In this thesis a concept has been developed which uses an automated test handler for placing the electronic devices on a test board.

1.2 Outline

In Chapter 2 an overview of the ESD phenomenon is presented. This chapter explains the charging process and the discharge event. At the end of this chapter, ESD protection and ESD damages are discussed. Chapter 3 presents the classic ESD test models, whereas Chapter 4 deals with the TLP testing approach. The information in these chapters originates from the literature.

In the course of this thesis an automated ESD test concept has been developed and is presented in Chapter 5. Chapter 6 presents details of the final ESD test approach. Especially, the test setup, Section 6.1, and the software used for controlling the test system, Section 6.2, are explained in detail.

Chapter 7 contains the final test results and in Chapter 8 a conclusion is drawn.

2 Fundamentals of Electrostatic Discharge

This chapter presents an overview of the electrostatic discharge phenomenon (ESD). ESD can compromise, damage or destroy an integrated circuit (IC) [1]. Therefore, it is very important to understand the processes which lead to this phenomenon. Based on this knowledge, protection strategies can be developed in order to improve robustness of microelectronic systems against ESD.

In daily life, when a person walks over a synthetic carpet, charge separation occurs due to friction (see Section 2.1.1). If the charged person touches a conductive material, for instance a metal car door, then an electrostatic discharge event happens. Usually the person feels it as an uncomfortable spark between the finger tip and the metal object.

In the following sections, the most important processes leading to ESD are presented. Section 2.1 deals with charging processes, the origin of ESD. Then the discharge phenomenon is explained in more detail (Section 2.2). The last sections provide information about damages (Section 2.5) caused by ESD and protection structures to prevent these damages (Section 2.4).

2.1 Electrostatic Charging

A prerequisite for an ESD event is charge-separation. The three most important charging mechanisms are triboelectric charging, direct charge transfer, and induced charging [2, chapter 2.2, p. 9f]. These charging mechanisms are discussed in the following sections.

2.1.1 Triboelectric Charging

Triboelectric charging can be observed when two uncharged objects are first put into contact and then get separated again. After separation, one object is negatively charged and the other one positively. This effect is illustrated in Figure 2.1. The classical method to demonstrate this effect is a well-known school experiment: When rubbing a glass rod with a wool towel, charge separation occurs, which can be verified with an electrometer [3, chapter 2, p. 2f].

The polarity of the charging process depends on the materials involved. A material can become positively or negatively charged, depending on the second material used. The triboelectric series provides a common used ranking of several materials, according to their charging. In Kaiser [3, chapter 2, p. 6] several different series are presented. Table 2.1 shows an exemplary triboelectric series.

The triboelectric series should be treated with caution: The ranking of the materials may vary in different series, because properties like the purity of a material or the surface roughness also impact the triboelectric charging process.

Triboelectric charging is a common issue in the semiconductor industry. During automated chip tests the packaged ICs are loaded in a gravity test handler. The chips are usually stored in their plastic shipping tubes. After starting the test procedure, the test handler flips the shipping tubes and the chips slide down the plastic tube. Due to this sliding, the chips are charged by the triboelectric effect.

2.1.2 Direct Charging

Direct charging or charge transfer happens when two objects with different charge get in contact. A charge transfer occurs from the higher potential to the lower one, until both objects have the same potential.

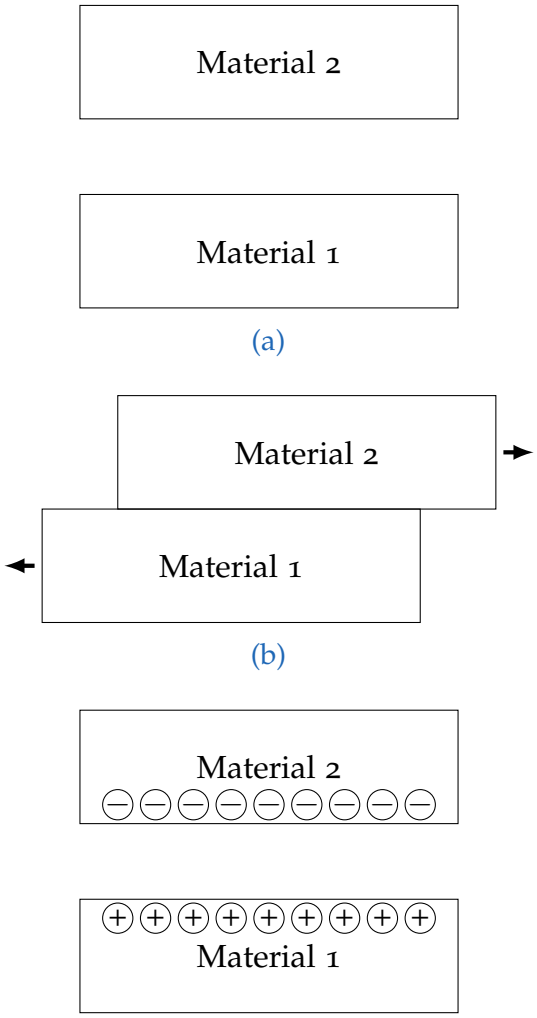

Figure 2.1: Illustration of the triboeletric effect. (a) Two materials prior to the experiment. (b) The materials are put into contact with each other. In this case they are also rubbed against each other. (c) The materials are get separated again. They are now charged.

Triboelectric Series	
positive +	Material
	Asbestos
	Glass
	Nylon
	Wool
	Lead
	Silk
	Aluminum
	Paper
	Cotton
	Steel
	Vulcanite
	Nickel and Copper
	Brass and Silver
	Synthetic Rubber
	Orlon
	Saran
	Polythene
	Teflon
	Silicon
negative -	

Table 2.1: Example of a triboelectric series, taken from [4, p. 642].

When an object is connected to a DC voltage source, charges flow to the object, until the initial potential difference is compensated. When the voltage source is removed afterwards, the object remains charged.

As described before, in an automatic gravity test handler the chips slide down the shipping tubes. When two chip packages with different charge get into contact, a charge transfer occurs [5, p. 403].

2.1.3 Induced Charging

This charging process is illustrated in Figure 2.2. A conceptual semiconductor test floor is shown. If a chip is brought in the proximity of a charged object, for example a computer monitor, the electrical field causes charge separation in the chip. If the chip is grounded afterwards, still in the presence of the electric field, a current pulse can be observed. First disconnecting from the ground and then switching off the computer monitor, leaves the chip charged. If it is grounded again, a current pulse can be observed, flowing in the opposite direction to the first one [5], [2, chapter 2.2, p. 10f].

2.2 Electrostatic Discharge

Electrostatic discharge (ESD) is the event of rapid charge transfer between two objects at different electric potentials. Once an electrical conductive path is established, a current flows from the object at higher potential to the object at lower potential. Figure 2.3 shows an example of this effect.

In case of ICs the discharge event causes a current between 0.1 A and 30 A within a very short time period (between 1 ns and 100 ns) [6, p. 5].

According to Amerasekera and Charvaka [2, chapter 2, p. 11] several different parameters influence the discharge event. Some of these parameters are the polarity, distance, shape, and material of the objects.

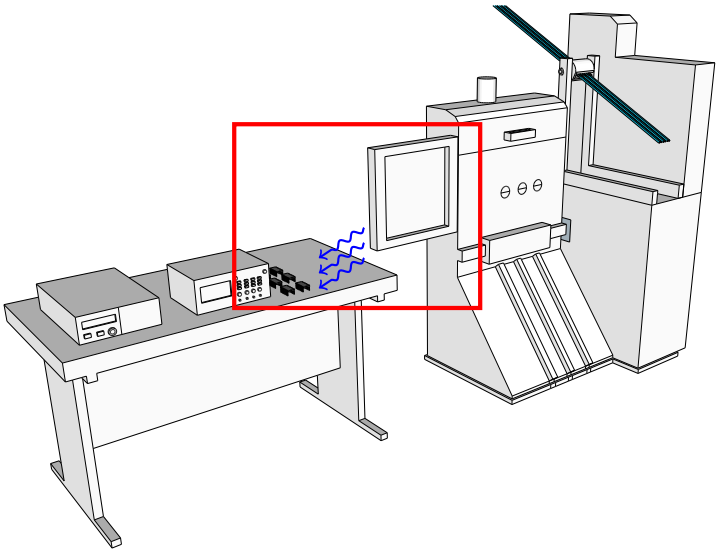

(a)

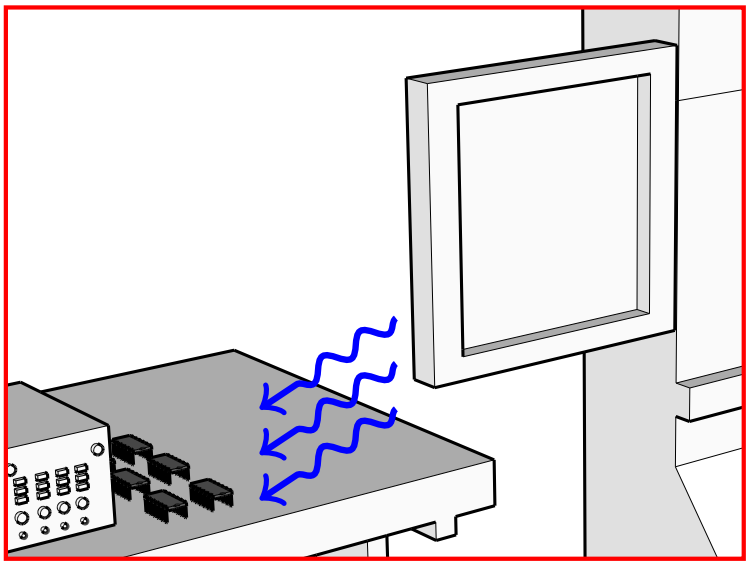

(b)

Figure 2.2: Illustration of an example for induced charging. Due to the presence of a computer monitor, the chips next to it are partially polarized. Grounding them results in a current pulse, and yet another, reverse current pulse can be observed, when the monitor is turned off again. (a) shows the test floor and (b) the chips and the charging process induced by the monitor.

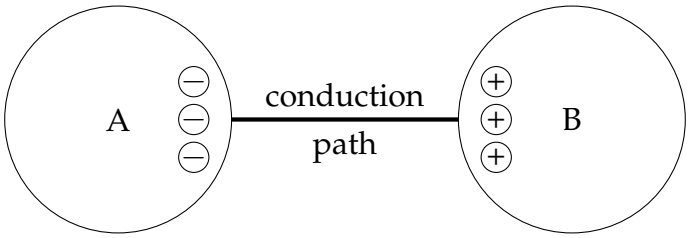

Figure 2.3: Preconditions for electrostatic discharge. The objects A and B are charged with respect to each other and a conduction path is established between them allowing for a current to flow.

2.3 Electrical Overstress

Stressing electronic devices or ICs beyond their electric ratings is called electrical overstress (EOS).

EOS can be classified, according to its character, into electrical over-current, electrical over-voltage and electrical over-power. The source for EOS is typically power generating equipment. EOS can have various effects on electronic devices like EMC, Latchup, EMI and also the previously described ESD.

A general EOS event can last up to seconds, whereas an ESD event takes place within a much shorter time period. The time period of ESD events ranges from a few nanoseconds to microseconds. Furthermore, ESD events are usually single, aperiodic pulses, whereas a general EOS is not restricted to a certain waveform; it can also be a periodic signal [7, 6ff].

2.4 ESD Protection

There are different strategies to protect electronic devices form ESD. The most frequently used protection approach is to provide an alternative, low ohmic bypass path for the ESD current, such that it does not flow through the sensitive components of the circuit.

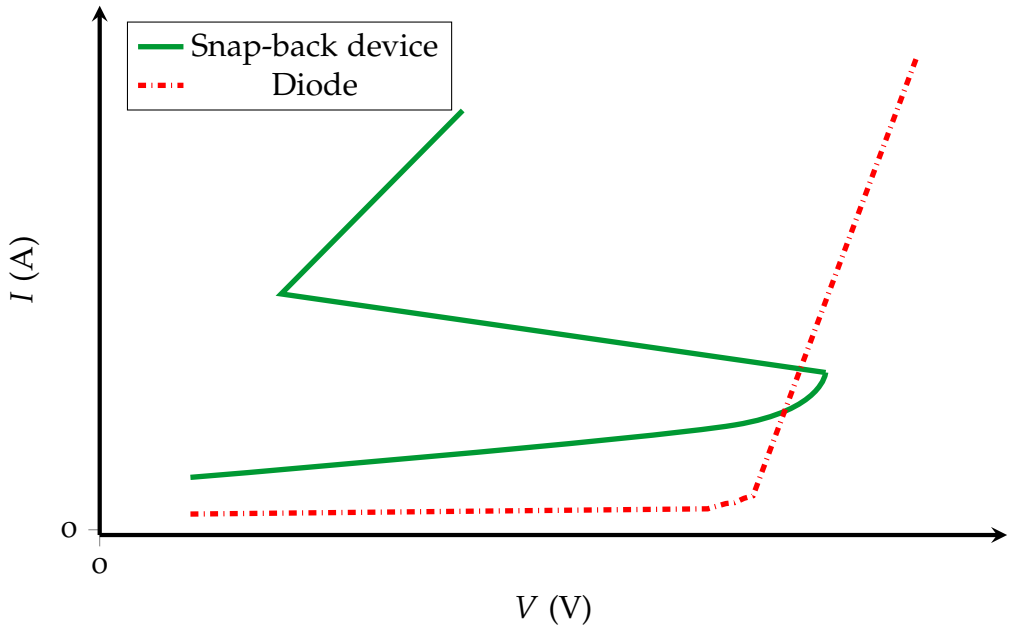

Figure 2.4: I-V curves for different protection structures.

2.4.1 Basic ESD Protection Devices

In the following sections, the basic structures to protect electronic devices from ESD are presented.

2.4.2 Diodes

ESD protection diodes make use of the avalanche breakdown effect to protect electronic devices. When the applied voltage at the diode reaches the breakdown voltage, a high current starts to flow through the diode. Therefore, the amount of current flowing through the device under protection is reduced. These diodes usually operate in reverse mode.

2.4.3 Snap-back Devices

A typical snapback device used for ESD protection is the grounded gate NMOS transistor (ggNMOS). The gate, the source and the bulk are connected to the ground, the drain is connected to the input or output pin. The solid line in Figure 2.4 shows a typical I-V curve of a snap-back device. If the snapback voltage is exceeded, the protection structure is activated and the voltage across the device is reduced.

2.5 Types of ESD Damages

In the following subsections a number of damages caused by ESD are described.

2.5.1 Junction Burnout

Junction burnout is a failure caused by ESD. In case of a long enough ESD event it is possible, that after the second breakdown excessive joule heating in the junction causes the contact metal to melt. As a consequence, metal spikes may form, which damage the semiconductor device. In Figure 2.5 this type of failure is demonstrated on a bipolar transistor [8, p. 122].

2.5.2 Oxide Breakdown

Another failure caused by ESD is oxide breakdown. In Figure 2.6 this type of failure is demonstrated on a MOSFET device. An ESD pulse can cause a very high electric field, which creates a conductive path in the gate oxide shorting the gate with the substrate. The heat build-up, due to the current, causes the oxide to melt along the path [5, p. 401],[9].

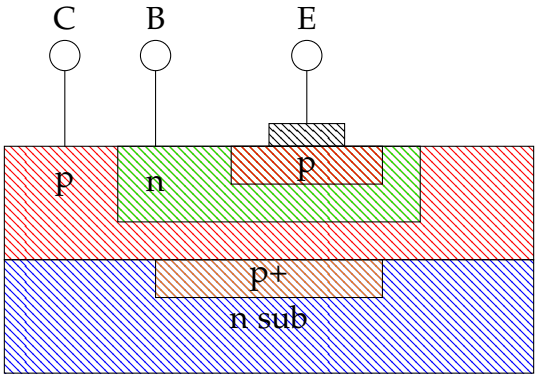

(a)

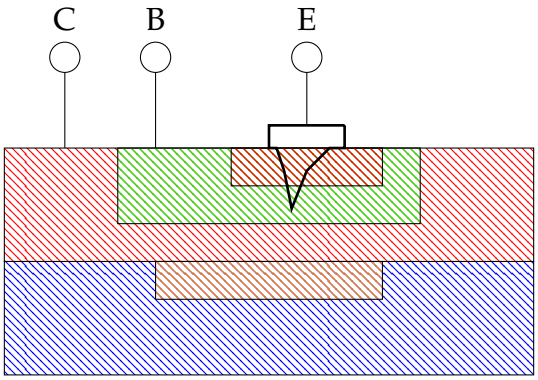

(b)

Figure 2.5: Illustration of junction burnout in a bipolar transistor. Due to an ESD event, the emitter electrode melts and the metal forms spikes, which penetrate into the device. (a) shows a working transistor and (b) a damaged one.

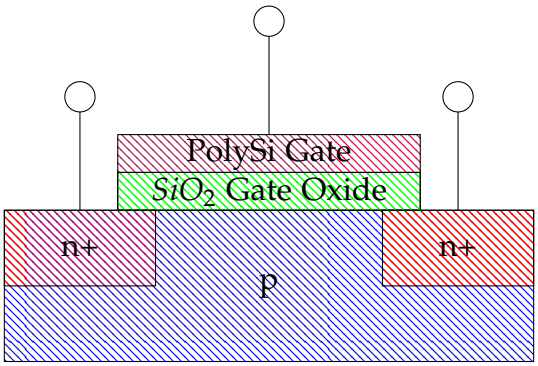

(a)

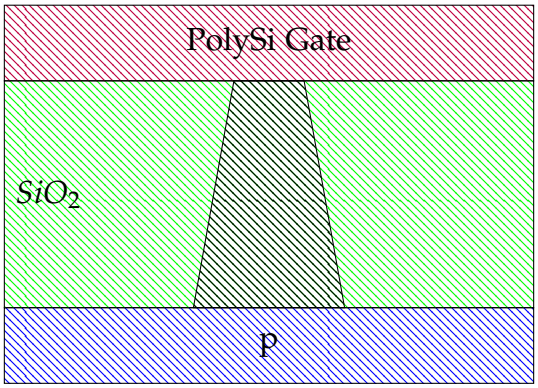

(b)

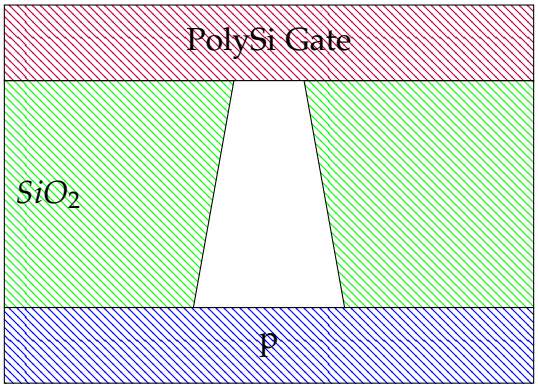

(c)

Figure 2.6: Illustration of oxide breakdown in a MOSFET. The high electric field associated with an ESD pulse provokes a conductive path in the gate oxide and therefore a short between the gate and the substrate. The oxide along the path melts, due to joule heating. (a) shows a working MOSFET, (b) the conductive path in the transistor during ESD and (c) the partially molten oxide.

2.5.3 Metallization Burnout

Metallization burnout is another possible failure caused by ESD. Very often this failure occurs after junction burnout or oxide breakdown. Figure 2.7 shows the damages on a MOSFET device. An ESD event causes a short between the contact electrodes, which leads to an increased current flow. As a consequence, the metal electrode melts and an open circuit in the metal layer remains [8, p. 122].

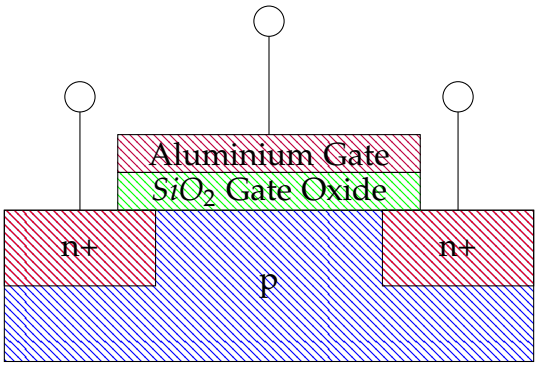

(a)

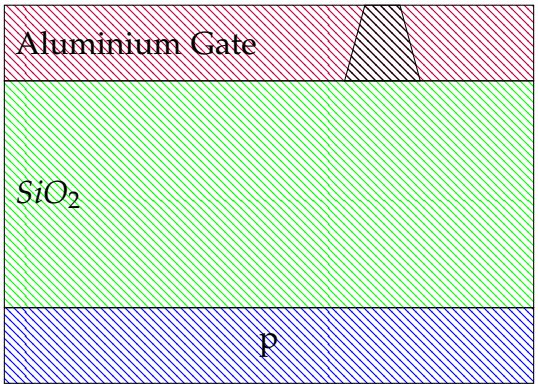

(b)

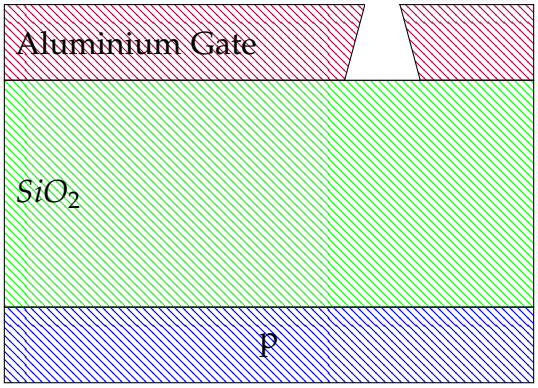

(c)

Figure 2.7: Illustration of metallization burnout in a MOSFET. An ESD event causes a short in the gate. The metal melts, due to joule heating, and leaves behind an open circuit. (a) shows a working MOSFET, (b) the short in the metal layer and (c) the open circuit.

3 Classic ESD Test Models

As discussed in the previous section (Section 2.5), ESD can damage electronic devices. Therefore, it is very important for the semiconductor industry to develop a test procedure which determines the sensitivity of electronic devices to ESD.

There are several institutions which developed and improved ESD test standards over the years.

- US Military Standard (MIL-STD)
- Electrostatic Discharge Association (ESDA)
- JEDEC Solid State Technology Association (JEDEC)
- Automotive Electronics Council (AEC)

These standards provide circuits and current waveforms for modeling ESD events. There are three major models for pass or fail classification of an electronic device, the Human Body Model (HBM), the Machine Model (MM) and the Charged Device Model (CDM). These models are explained in more detail in the following sections [10, 189ff].

3.1 Human Body Model

One of the most often used and oldest ESD stress models is the Human Body Model (HBM). As the name suggests, it models the event that a charged person touches an electronic device. When the person gets in contact with chip pins, an ESD event occurs [10, 191ff].

Figure 3.1 shows a simplified equivalent circuit for an HBM tester. A capacitor with 100 pF in series with an 1500 Ω resistor simulate the charged

human body. The stressed device is placed in a socket in series with the resistor and the capacitor.

The current waveform is verified by using a short circuit and a 500 Ω resistor. The current waveform in a short circuit is shown in Figure 3.2.

An HBM ESD is a single polarity event. The HBM ESD standard is fulfilled, if both polarities pass the test procedure. In order to test all current paths on a chip, it is necessary to test all pin combinations. Using automated tester handlers all pin combinations can be tested in a reasonable time [7, p. 134].

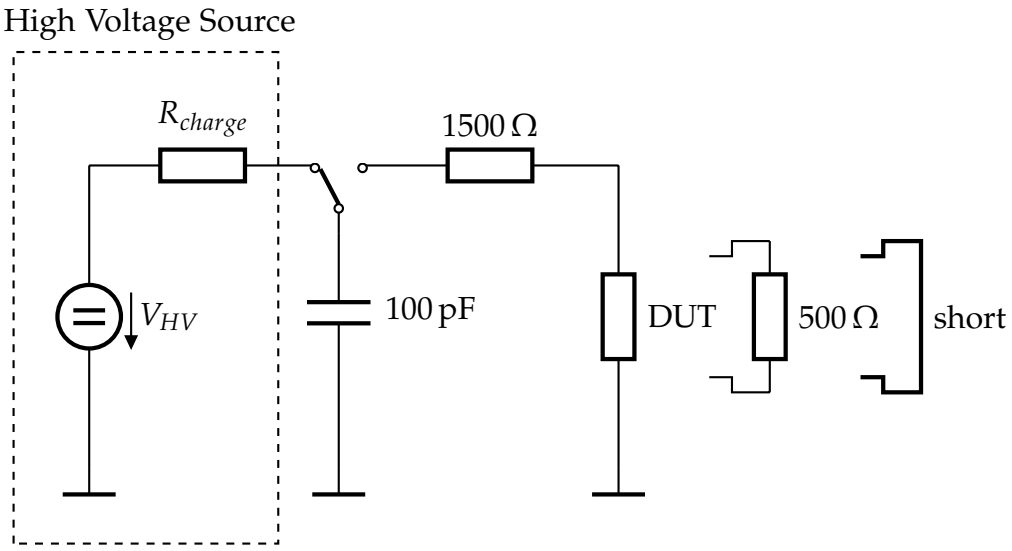

Figure 3.1: Equivalent circuit for HBM, adapted from [10, p. 192].

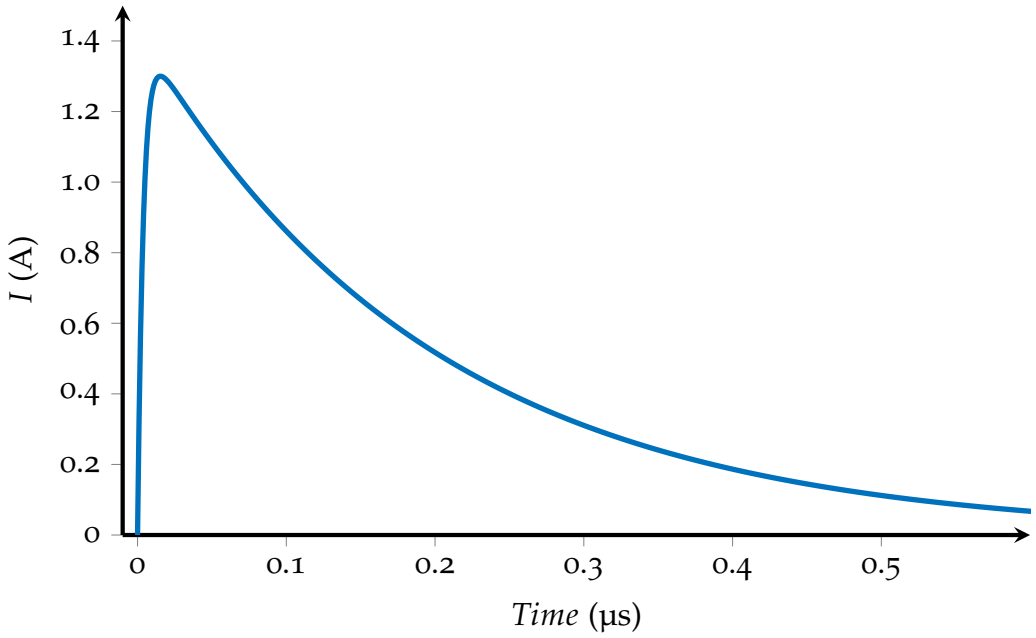

Figure 3.2: HBM current curve for a short circuit.

3.2 Machine Model

The Machine Model (MM) is a modified version of the Human Body Model. In contrast to the HBM, which deals with the discharge of a human body to an IC, this model describes the discharge of a charged machine. The resistance of the conduction path is much smaller than in the HBM, because the conductive material usually is a metal. Therefore, the peak current is much higher than in HBM for the same pre-charge voltage.

In Figure 3.3 the equivalent circuit for this model is presented. In comparison to Figure 3.1 for the HBM, the capacitor has now 200 pF and the resistor 0 Ω, because a metal is a much better conductor than the human body. In Figure 3.6 the current waveform for a short circuit is presented. The current oscillates due to the parasitic inductance of an MM tester [10, 194f].

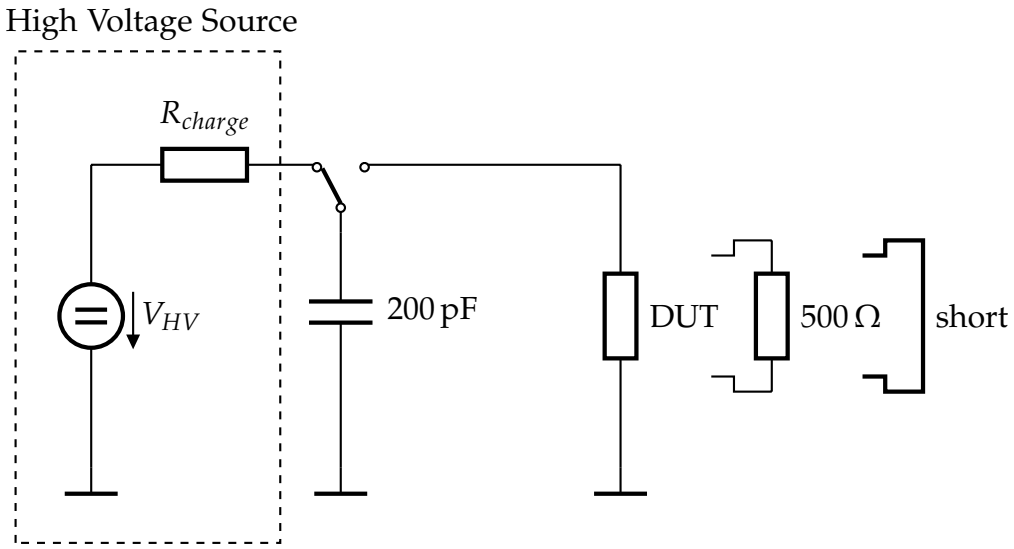

Figure 3.3: Equivalent circuit for MM, adapted from [10, p. 195].

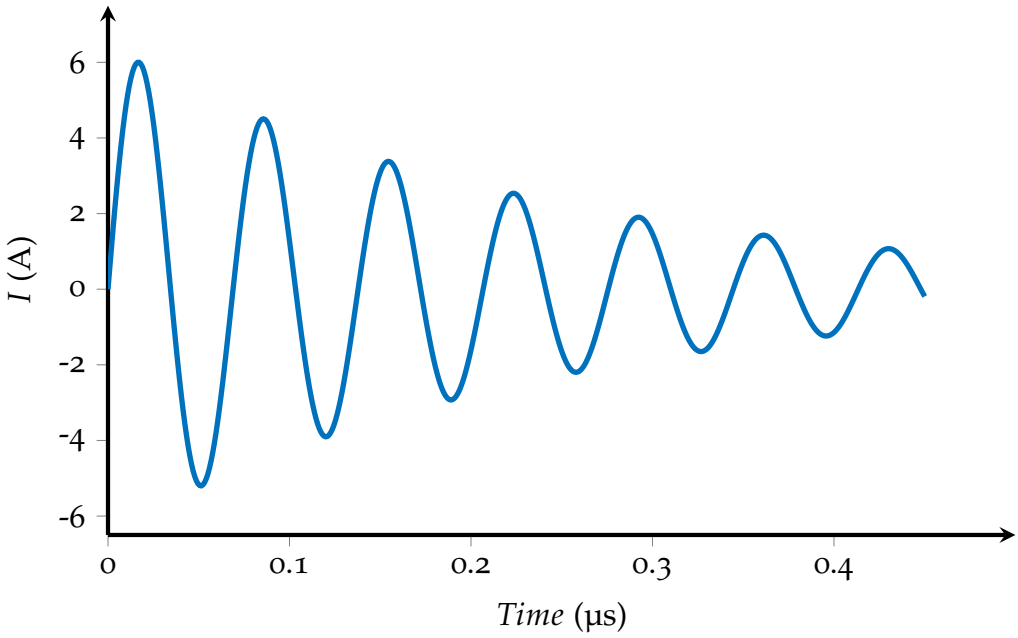

Figure 3.4: MM current curve for a short circuit.

3.3 Charged Device Model

As discussed in Section 2.1.1 and Section 2.1.3, a device can be charged by induction and by the triboelectric effect. An example for the triboelectric effect, which is also very important in practice, is the charging of chips when they slide down the shipping tube. This happens in automated gravity test handlers. A test handler flips the shipping tube, in order to place the ICs in the handler feeder. To be able to cover such events, the Charged Device Model (CDM) has been introduced.

When the pin of a charged device gets in contact with a conductive object, an ESD event occurs at this pin. Due to the low resistance path, a high current flows (several Ampere). The duration of such an ESD event is much shorter than in the MM and HBM. Figure 3.6 shows a typical current curve for the CDM [10, 196f].

In practice, there are two test methods for a CDM event, the socket and the non-socket device test method. Figure 3.5 shows a sketch of the non-socket device test method. The device under test is placed on a grounded plate, such that its pins are pointing straight up in the air (dead bug position) [11, 405f].

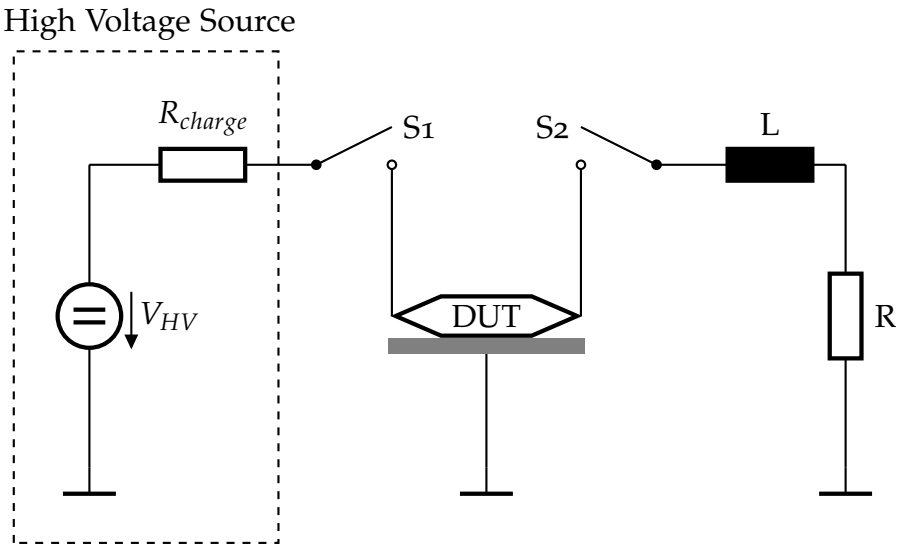

Figure 3.5: Sketch of the non-socket device test method for CDM, adapted from [10, p. 197].

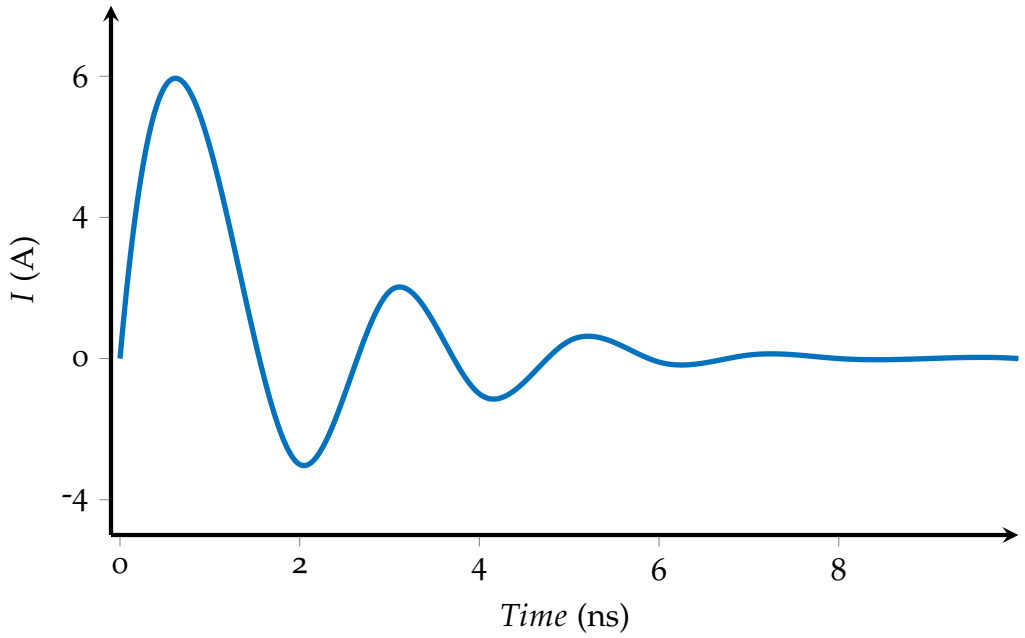

Figure 3.6: CDM current curve of a 500V ESD, adopted from [10, p. 197].

4 TLP-Characterization of ESD Protection

The CDM, MM and HBM produce different types of damages. Even testers of the same ESD model, but from different manufactures do not always yield reproducible results. In Zur Nieden, Arndt, Edenhofer, *et al.* [12] it is shown, that standardized ESD testers for these models produce different current peaks. Therefore, the so-called Transmission Line Pulse (TLP) testing is often favored over the classic ESD models.

TLP uses rectangular pulses for stressing the electronic devices. As already mentioned in Chapter 3, the classic ESD test methods provide a fail or pass classification only. TLP offers the possibility to get detailed information on the device under test (DUT) response to ESD events.

The following sections present the fundamentals of TLP testing, including the basic approach and a more detailed explanation of the TLP generator, as well as the Wunsch-Bell curve [11, 405f], [10, 196f].

4.1 Transmission Line Pulse Testing

In the TLP test system a transmission line is charged by a high voltage source. After the transmission line has been charged up, a switch is closed, the transmission line discharges and thereby generates a square wave pulse. This pulse stressing technique is used to obtain failure levels and characterization data of the test devices [13].

The TLP testing method was first described by Maloney and Khurana [14]. In Section 4.1.1 the principle of TLP testing is explained. For a better

understanding in Section 4.1.2 the generation of transmission line pulse is presented.

4.1.1 Basics of Transmission Line Pulse Testing

In Figure 4.2 a basic setup for a TLP test system is illustrated. The test system consists of high voltage source, which charges a transmission line through a resistor. Usually a coaxial cable is used as a transmission line. After the transmission line reached a predefined voltage level, switch S_1 is closed and the coaxial cable is discharged. This causes a rectangular pulse. The pulse width of this pulse can be controlled by the length of the transmission line.

The pulse is applied to the DUT. During the test the current through and the voltage across the device are captured by an oscilloscope. A typical current and voltage curve is shown in Figure 4.1. It is common practice to take measurement points at the end of the pulse and average them, in order to get rid of the transients and remaining time dependencies. These averaged current and voltage values are then plotted against each other in a current-voltage (I-V) curve.

Starting with low pulse heights, the voltage is increased successively until the device is damaged. After each test loop the leakage current is measured. When leakage current exceeds a predefined threshold, the device is considered as damaged. By using this information it is possible to generate a Wunsch-Bell curve, which is explained in more detail in Section 4.2 [10, 198ff].

4.1.2 Transmission Line Pulse Generator

The basic principle of an TLP generator is explained in Simbürger, Johnsson, and Stecher [15]. The basic setup of a TLP generator is presented in Figure 4.2. The transmission line is characterized by the impedance Z_0 (which is the overall characteristic impedance: $Z_{TLP} + Z_{TL_2} + Z_{DUT}$) and the line length L.

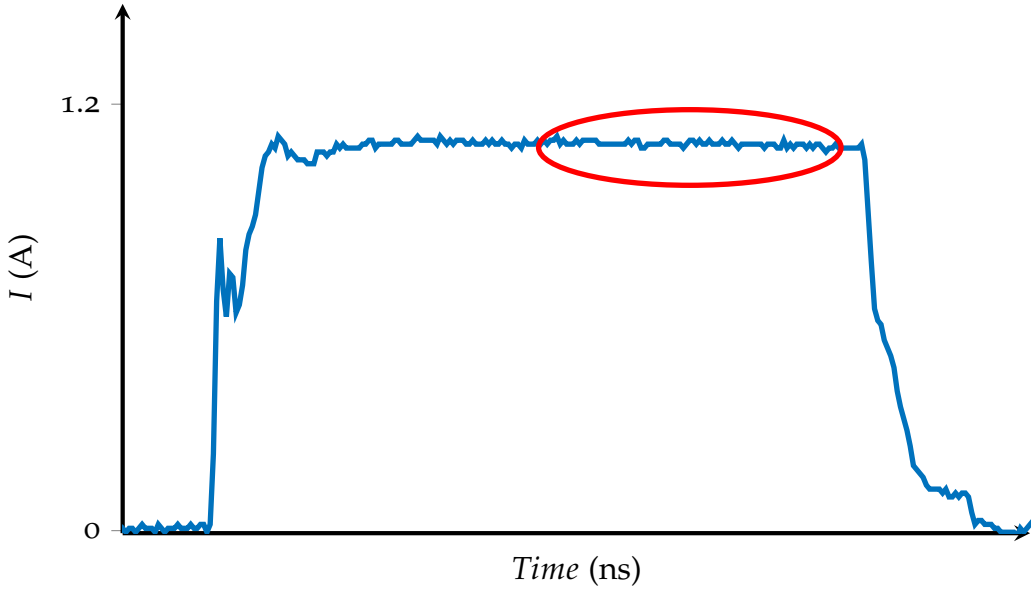

Figure 4.1: Exemplary transmission line pulse. Date points between 50% and 80% of the pulse width (that region is marked with an ellipse) are averaged and used for generating the I-V curve.

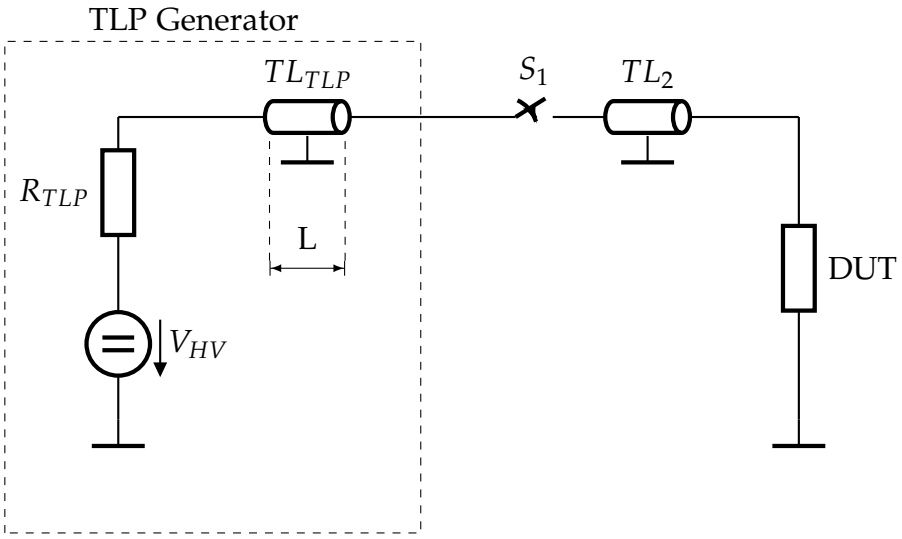

Figure 4.2: Simplified TLP generator.

The generator is ready for use when the transmission line is charged to a specific voltage. The resistance of R_{TLP} has to be much larger than Z_0 of the transmission line, otherwise the source would deliver an excessive amount of energy during the time when the switch is closed. This is necessary to get a well formed square pulse. After the switch is closed, the wave propagates to the end of the transmission line which is terminated by a high ohmic resistance (ideally with $R \to \infty$). Due to the high resistance, the wave is almost entirely reflected and propagates back the transmission line. In Figure 4.3 the generation of the transmission line pulse is illustrated.

Figure 4.3a shows the pre-start condition for $t < 0$ s. The high voltage source charges the transmission line TL_{TLP} up to the voltage level V_{HV}. The transmission line TL_2 is disconnected from the generator, since switch S_1 is open.

Figure 4.3b illustrates the start condition. After the switch S_1 is closed, the voltage at the right-hand side of TL_{TLP} becomes $\frac{V_{TLP}}{2}$ since the wave impedance of TL_{TLP} and TL_2 are equal.

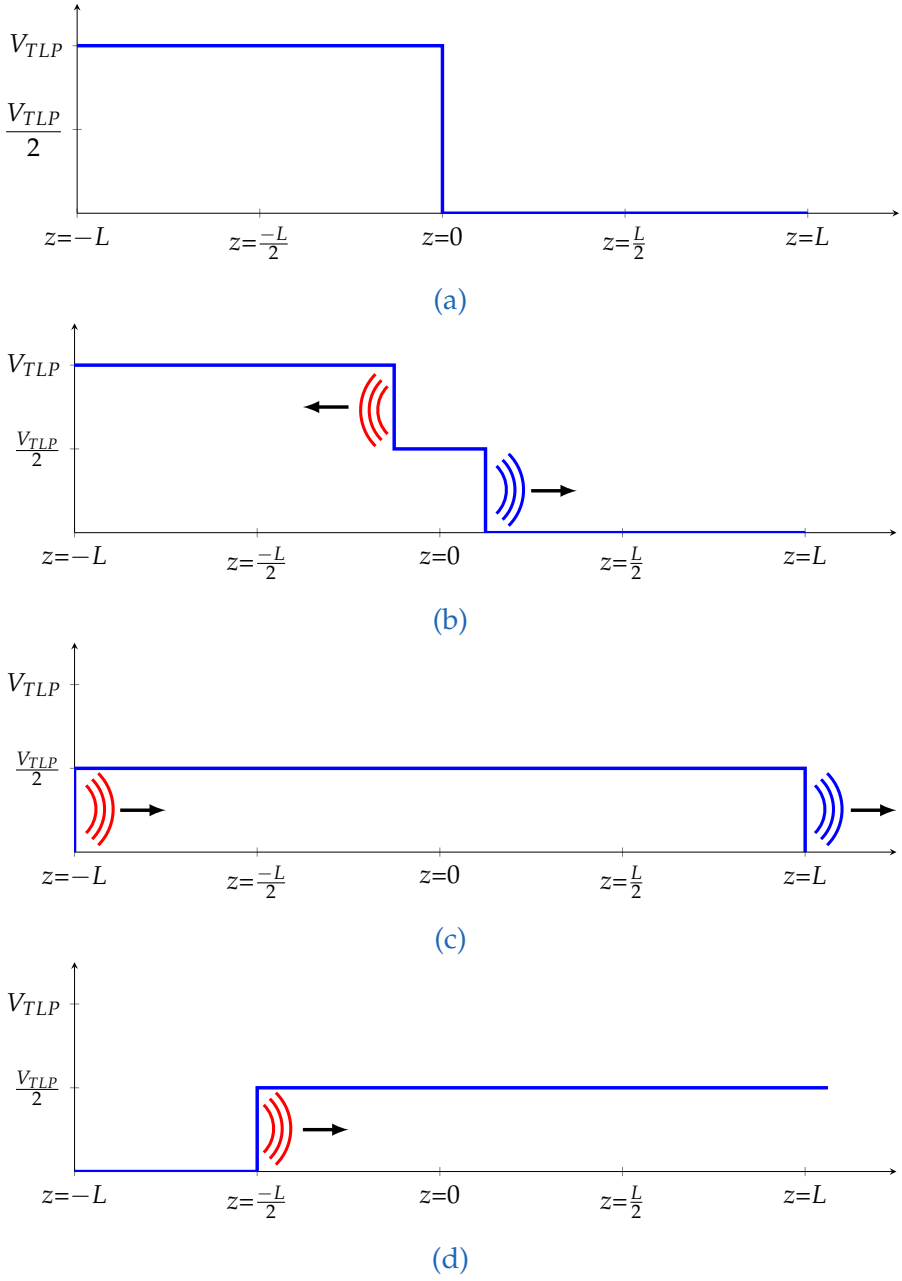

Figure 4.3: Evolution of a rectangular pulse from a TLP generator, adapted from[15].

Two waves propagate along the transmission line in opposite direction. The red wave moves in negative z direction with the voltage $-\frac{V_{TLP}}{2}$. The blue one travels in the positive z direction with a voltage $\frac{V_{TLP}}{2}$.

Figure 4.3c shows the arrival of the red wave at the end of TL_{TLP}. Since this is an open end, the wave is reflected with the opposite polarity.

Figure 4.3d illustrates the further traveling progress until the transmission line is discharged again.

This demonstrates that the wave generated by a TLP generator travels a distance twice the length of the transmission line. Therefore, the pulse width can be varied by changing the length of the transmission line TL_{TLP}.

4.2 Wunsch Bell

Wunsch and Bell [16] investigated the power to failure of diodes and transistors and described a model for thermal failure. According to [17, p. 59], [16], Wunsch and Bell noted the following:

- The electronic component is capable of sustaining a higher power, if it is biased in the forward direction.
- If the applied pulse lasts longer, the necessary power to damage the component is lower.
- The power to failure as a function of the width of the incident pulse does not depend on the polarity.

Wunsch and Bell observed a specific behavior of the power to failure depending on the pulse width. Figure 4.4 shows the Wunsch-Bell curve with three typical regions [18, p. 31], [16]:

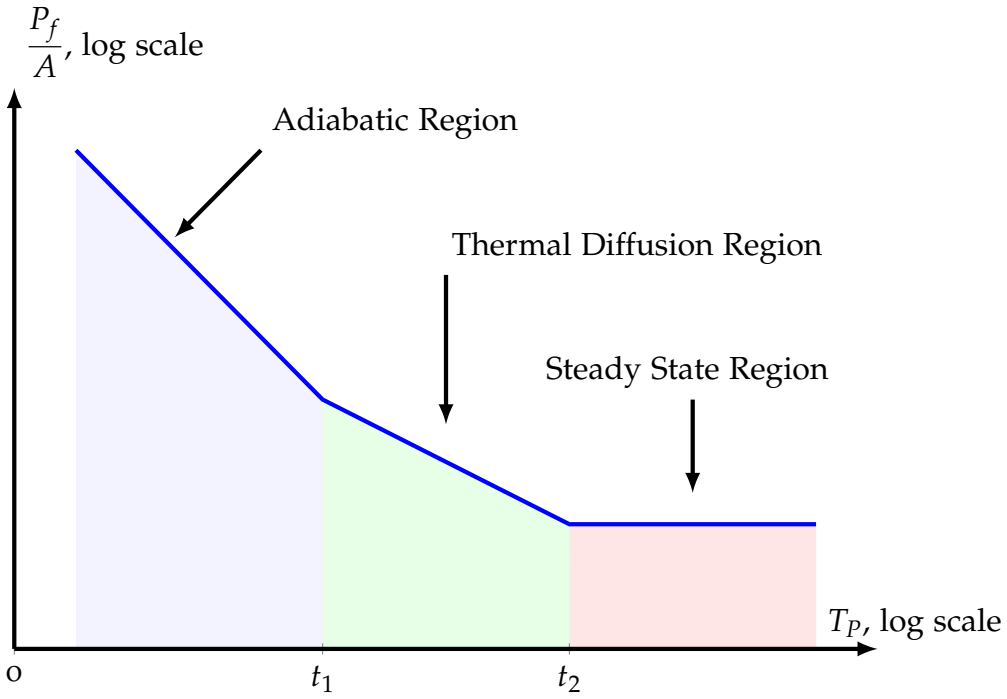

Figure 4.4: Wunsch-Bell curve.

- Adiabatic Region: For times $t < t_1$ the heat cannot be dissipated and a constant energy is required to damage the component. Thus the power to failure is proportional to $\frac{1}{t}$.
- Thermal Diffusion Region: For $t_1 < t < t_2$ the power to failure goes with $\frac{1}{\sqrt{t}}$.
- Steady State Region: For pulse widths $t > t_2$ the power to failure approaches a constant value. This means that the amount of power dissipated from the component equals the amount of power generated.

5 Development of a TLP Test Concept

Modern ICs consists of several hundred pins. In order to test all pin combinations in a reasonable time, an automated TLP test approach is needed. In Section 5.1 different TLP implementation are discussed and in Section 5.2 an automated TLP test concept is presented.

5.1 TLP Implementations

5.1.1 TLP 500

In Figure 5.1 a typical TLP 500 setup is presented. The resistor network is used to cancel the reflections between the open end of the transmission line and the stressed device. The 55 Ω and 500 Ω resistors form a termination network to prevent reflections back into the TLP generator. This test setup is mainly used for HBM events characterizations, therefore the pulse width is 100 ns.

The current through and voltage at the DUT is recorded by an oscilloscope. Switch S_2 is used to disconnect the DUT from the pulse generator and to connect it to the source measurement unit (SMU). The SMU is used for acquiring the leakage current from the device after each stress test [2, 53ff].

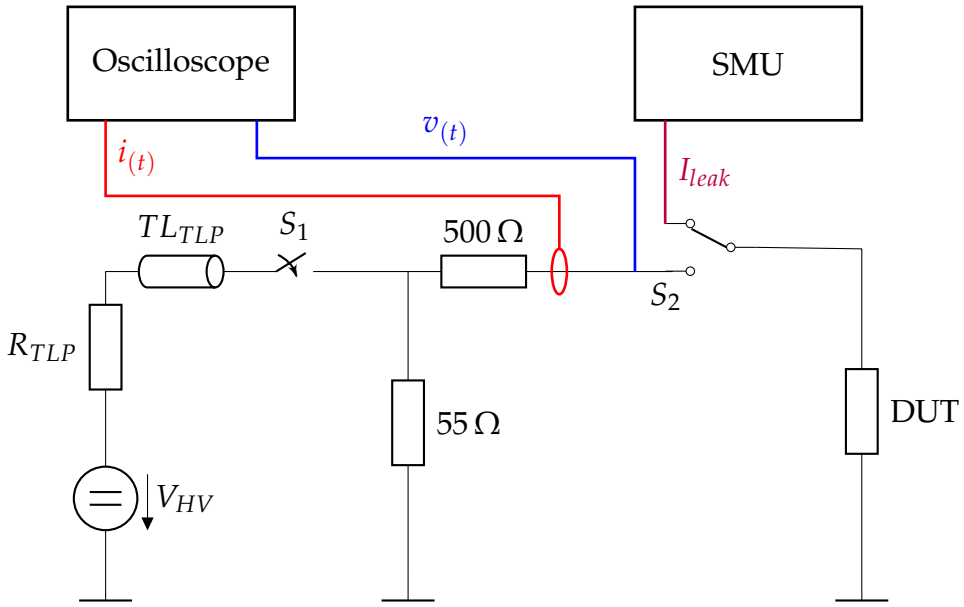

Figure 5.1: TLP 500 setup, adapted from [2, p. 51].

5.1.2 Time Domain Reflection-TLP

In this TLP setup the incident and the reflected wave at the device is measured by an oscilloscope. When the incident wave reaches the DUT, a wave, depending on the relation between the impedance of the DUT and the transmission line, is reflected. A Time Domain Reflection-TLP (TDR-TLP) setup is shown in Figure 5.2 [2, 53ff].

5.1.3 Time Domain Transmission-TLP

In this TLP setup the first oscilloscope (Oscilloscope 1) is used to capture the incident and reflected wave. Another oscilloscope (Oscilloscope 2) records the transmitted wave. The setup is illustrated in Figure 5.3 [2, 53ff].

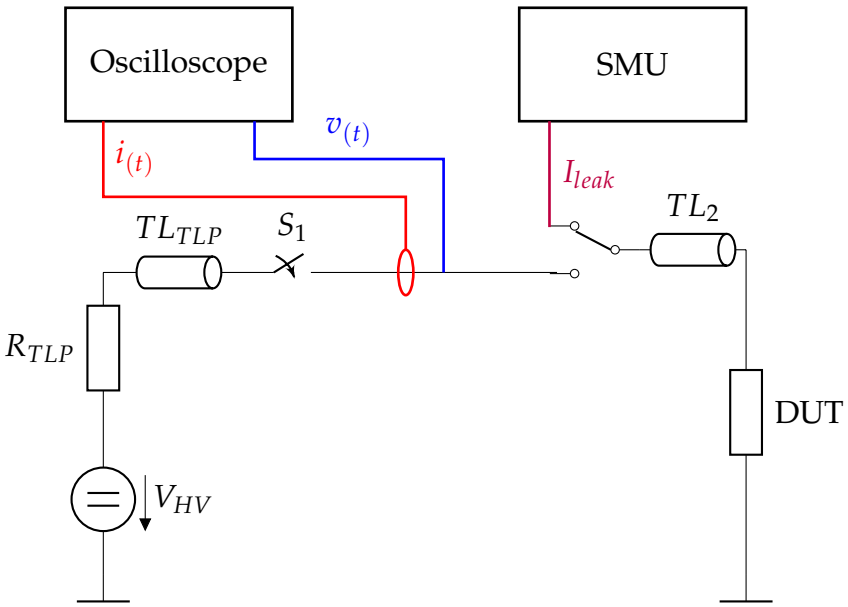

Figure 5.2: TDR-TLP setup, adapted from [2, p. 51].

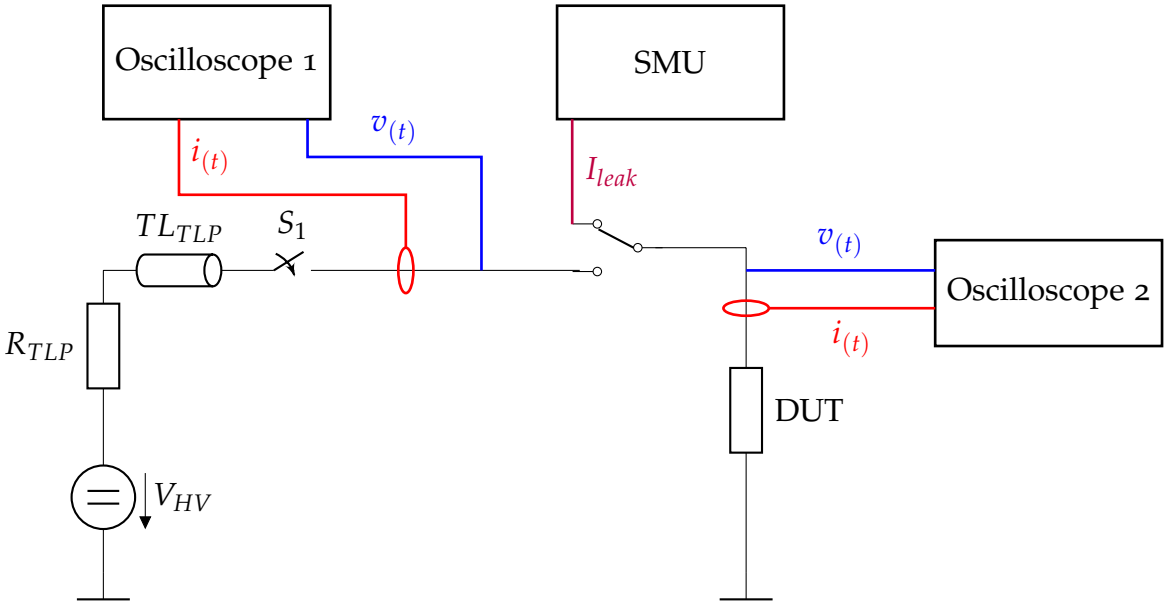

Figure 5.3: TDT-TLP setup, adapted from [2, p. 52].

5.1.4 Time Domain Reflection and Transmission-TLP

This setup is very similar to the TDT-TLP setup. Again two oscilloscopes are used for capturing the incident, reflected and transmitted wave. The DUT is now placed in series with the discharge path. Figure 5.4 shows the TDRT-TLP setup [2, 53ff].

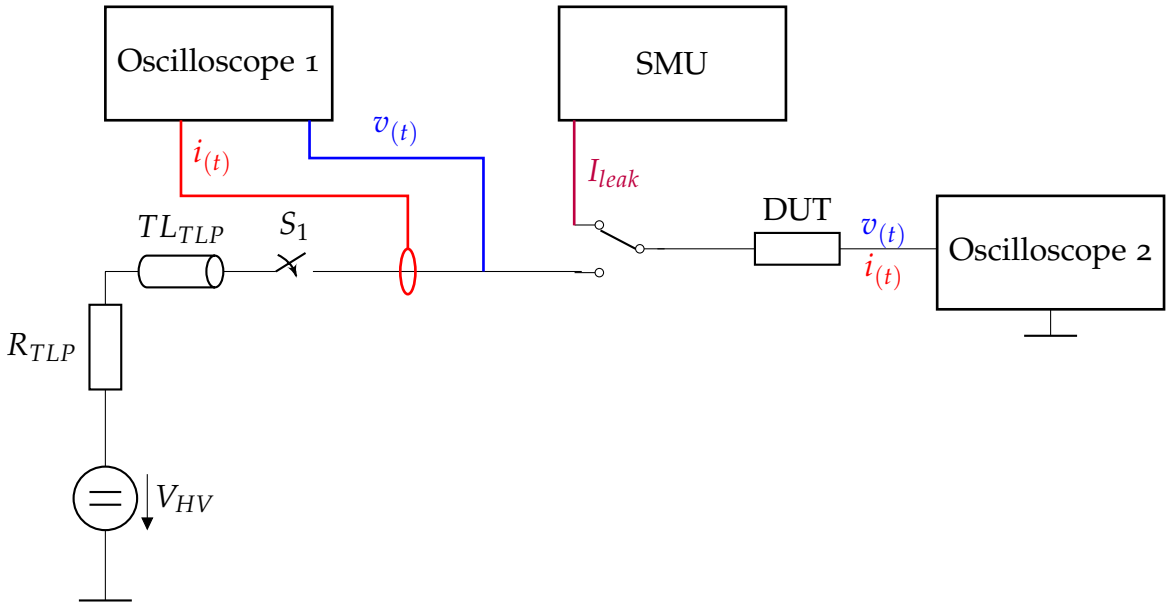

Figure 5.4: TDTR-TLP setup, adapted from [2, p. 52].

5.2 IC Test Handler

In order to develop a fast and robust ESD test setup, it is necessary to use an automated test handler. There are three types of test handlers, which are used for different electronic levels:

- System level
- Component level
- Wafer level

This work will focus on the component level. A component level test handler is used for placing the devices on a test board (load board), which is the interface for test and measurement equipment.

Commercial test handler suppliers provides two types of chip package test handlers. The first one are so called pick and place handlers, which are able to pick up devices from a specific location (usually there is a feeder tray near the handler) and place the component on the test board.

The second type is a gravity handler, which is intended for our concept. The next sections present a detailed overview of operating principle and the required peripheral [19].

5.2.1 Operating Principle of a Gravity Test Handler

ICs are usually stacked in plastic shipping tubes. These shipping tubes are placed in the tube shuttle of the gravity handler. At the beginning of the test procedure, the tester flips the shipping tubes. Due to the gravitational force, the devices slide down the shipping tubes. Some machines are equipped with air blowers in order to prevent lighter packages to be stuck in the tubes [19, 3f].

The chips slide down into the feeder shuttle. This part of the machine moves the ICs, through a temperature chamber, to the contact sites. The temperature chamber allows the heating or cooling of the chips to a predefined temperature.

For testing the devices, it is necessary to manufacture loadboards. A loadboard is a printed circuit board (PCB), which provide an interface to test and measurement equipment [19, p. 4].

Tested chips are moved in the unload trays. It is possible to separate the chips in different trays. A mock-up of the gravity test handler is presented in Figure 5.5. The most important parts of the handler are shown in Figure 5.6.

This concept uses the MT93xx Gravity Handler from Multitest. This handler is able to work with the following SO packages: SO150, SO209, TSSOP173, TSSOP240, MSO118, SO300, SO370.

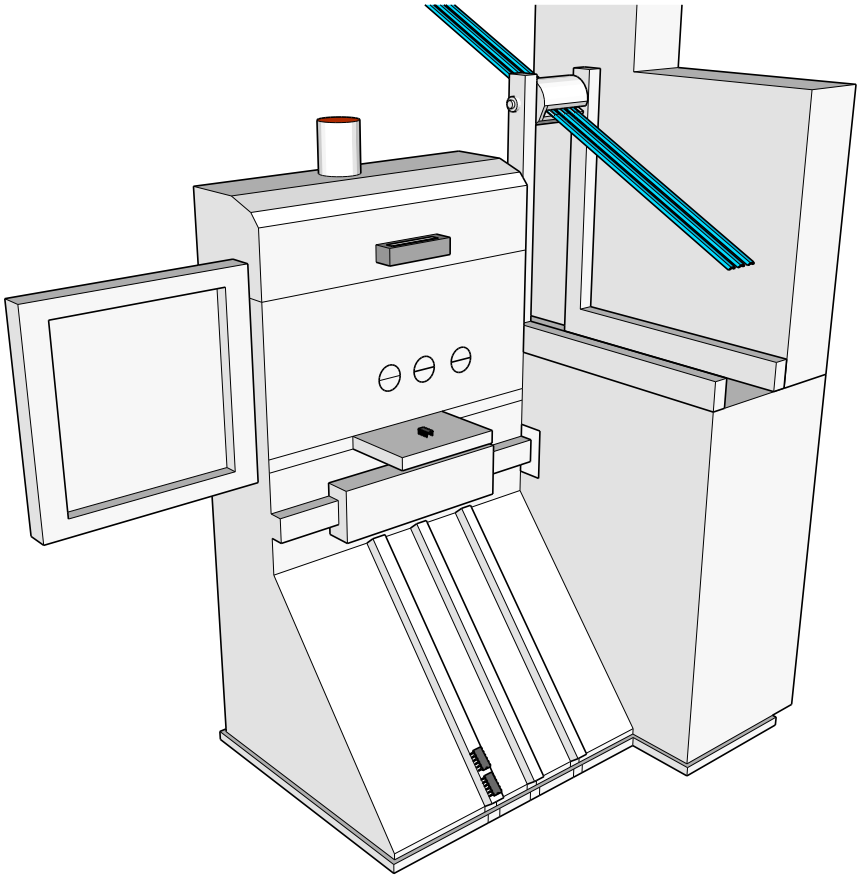

Figure 5.5: Mock-up of the gravity test handler.

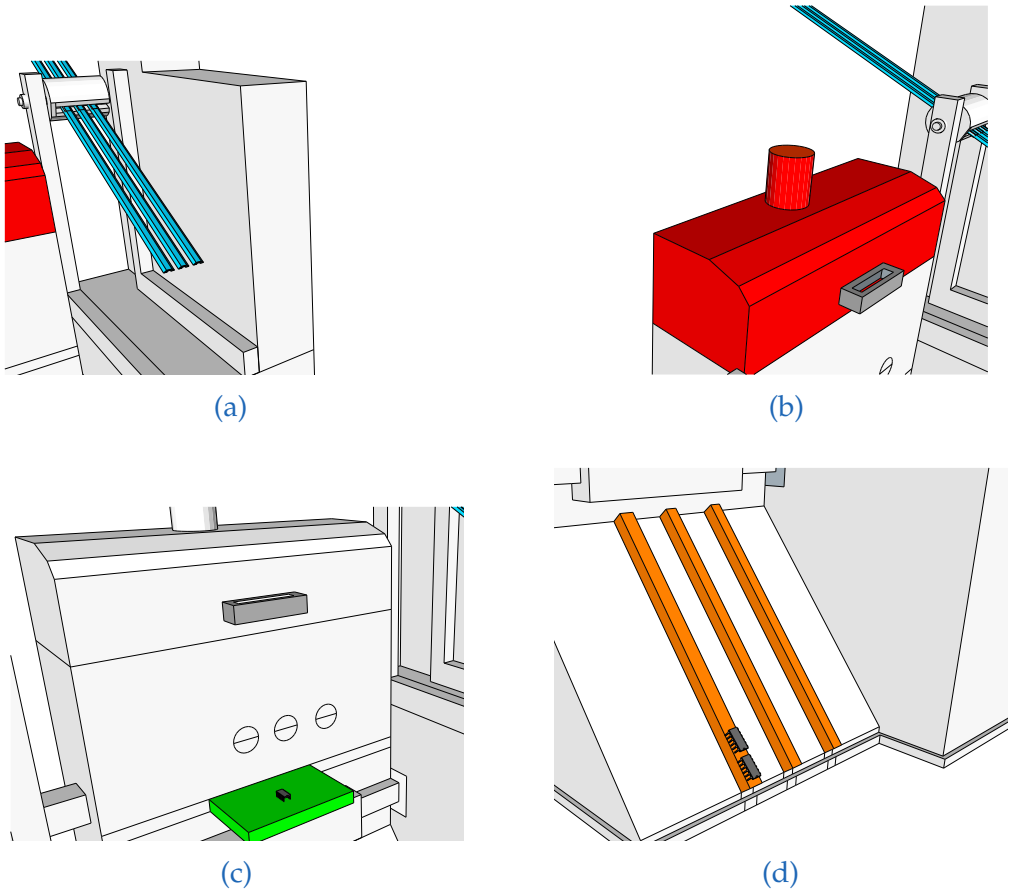

(a) (b) (c) (d)

Figure 5.6: Most important parts of this handler type. (a) shows the shipping tubes, which contain the electronic devices. (b) After flipping the tubes, the devices are passes to the heating chamber. (c) During the TLP test the device is placed on loadboard. (d) After the test the chips are placed in the unload trays.

5.3 Communication Bus

The TLP test system is controlled by a personal computer (PC). The PC communicates with the measurement equipment via a communication bus. Therefore, it is very important for choosing a reliable and cost effective communication system.

There are several options for choosing the communication bus. In the following the most promising are discussed.

Universal Serial Bus (USB) The Universal Serial Bus is a very popular bus protocol used to connect PC infrastructure with electronic devices. Most of the modern test measurement equipment support USB-B. The cable length is limited to several meters and especially USB-B cables have limited shielding. Another issue is the limited USB ports of a typical PC [20, p. 18].

General Purpose Interface Bus (GPIB) The General Purpose Interface Bus was originally introduced by Hewlett-Packard in the 1970s. Therefore, the bus is also known as HP-IP, which can be seen on older electronic devices. Due to the fact that the bus uses a physical parallel interface it is necessary to use a USB to GPIB converter in order to use that communication method with modern PC. An advantage of GPIB is the capability to stack the physical cables together, which means you only need one USB to GPIB converter. In order to talk with each instrument each devices must be assigned with an address. According to the IEEE 488 Standard it is possible to connect up to 14 electronic devices [21].

5.4 Prototype Setup

In Figure 5.7 a concept of our prototype TLP test setup is presented. The test system in controlled by a PC. The PC uses the GPIB for communicating with the test and measurement equipment. In Figure 5.8 the communication flow is shown. A National Instrument USB to GPIB converter is used [22].

The MT93xx Gravity Handler is used to automatically place the devices on the loadboard. The loadborad is a self-made PCB with a device socket (depending on which package is currently used). These loadboards can be adapted to fulfill the test requirements. The design and layout of the loadboard depends on the TLP test setups which are presented in Section 5.1.

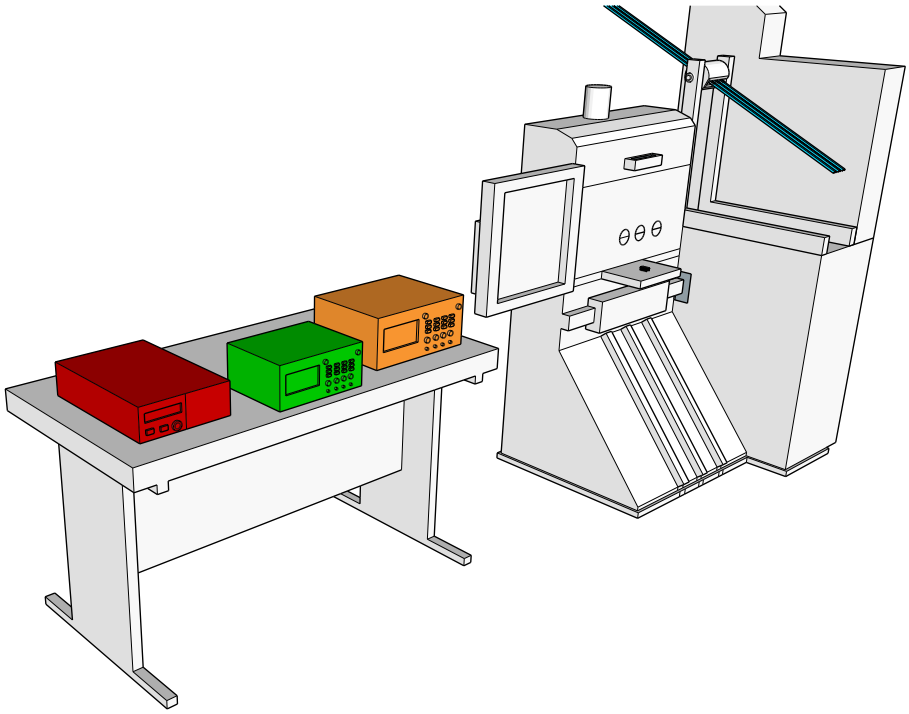

Figure 5.7: Sketch of the automated TLP test system. An oscilloscope records the current and voltage curves. The SMU is used for leakage current measurements. The TLP generator stresses the DUT.

For recording the current and voltage curves an oscilloscope is used. The data is first stored in the oscilloscope buffer and is then sent to the PC after each stress event. A SMU records the leakage current of the DUT.

The test chip is stressed until the maximum leakage current threshold is reached. Then the device is detached from the loadboard by the test handler and the next device is placed in the loadboard.

By collecting measurement data it is possible to produce I-V curves and a Wunsch Bell characteristic for the devices. By using the automated TLP test system it is possible to evaluate a large number of integrated circuits.

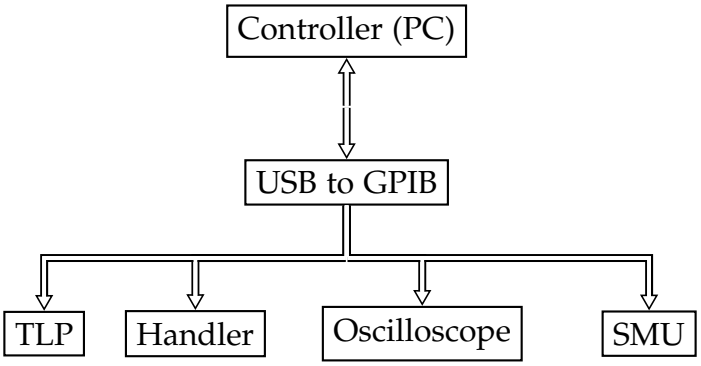

Figure 5.8: Communication setup for the automated TLP test system.

6 Realization of TLP Test System

In this chapter the realization of the developed TLP test system is described. It is divided into two main sections. Section 6.1 deals with the test setup. The schematic for the setup is presented in Section 6.1.1. The automated gravity test handler, presented in Section 5.2 is not used in the course of the measurements, because it is compatible only with a single chip package type. Section 6.2 contains a description of the implemented software for controlling the measurement equipment.

6.1 TLP Test Setup

In this section the TLP test system is described.

6.1.1 Schematic

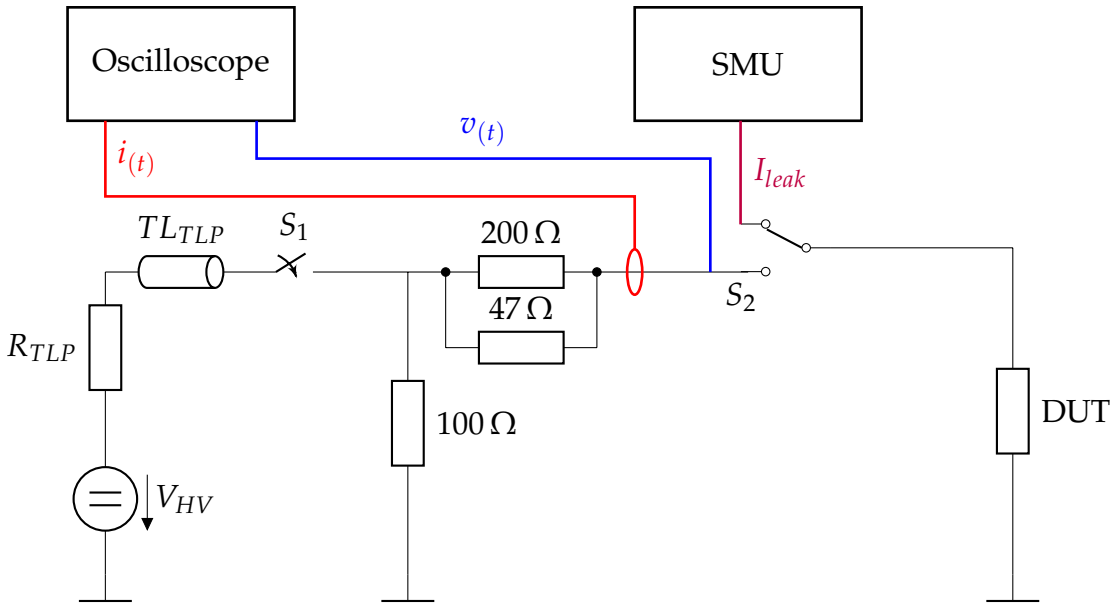

Figure 6.1: Schematic of the TLP test system.

6.1.2 Test PC

The developed software is tested on a Windows 10 PC. The hardware configuration is shown in Table 6.1. The software should be compatible with all Windows versions, as long it supports Matlab 2015a.

PC Data			
Manufacturer	Model	Operating System	Interfaces
Lenovo	T450s	MS Windows 10	USB

Table 6.1: Data of the used PC.

6.1.3 Measurement Equipment

Oscilloscope In order to observe the current and voltage pulse during the TLP test, an oscilloscope is needed. Therefore, a MSO6054A with a CT-1 current probe is used. In Table 6.2 the data of the used oscilloscope is presented.

Oscilloscope Data				
Manufacturer	Name	Bandwidth	Sample rate	Interfaces
Keysight	MSO6054A	500 MHz	4 Gs/s	USB, GPIB

Table 6.2: Data of the used oscilloscope.

Source Measurement Unit A source measurement unit from the ADC Corporation is used for leakage current measurement. The data of the used SMU is presented in Table 6.3. The GBIP address is set to 7.

Source Measurement Unit Data				
Manufacturer	Name	Voltage Range	Current Range	Interfaces
ADCMT	6241A	0 to $\pm$32V	0 to $\pm$500 mA	GPIB

Table 6.3: Important facts of the source measurement unit taken from [23]

6.1.4 Test Equipment

A TLP generator from NoiseKen is used for stressing the DUT. The pulse voltage and the pulse width can be manually adjusted. The TLP generator is triggered manually by a push button. The data of the used TLP generator is presented in Table 6.4.

Transmission Line Pulse Generator Data			
Manufacturer	Name	Voltage Pulse Range	Interfaces
NoiseKen	INS-429A	0 to 2000 V	-

Table 6.4: Important facts of the oscilloscope.

6.2 Software

The numerical computing software Matlab is used for controlling the equipment, acquiring the data and for data post processing. The reason for choosing this software solution is that Matlab is widely used in academic research groups. Therefore, it is guaranteed that the code which is produced during this thesis can be easily extended.

Another reason for using this product suite are the strong capabilities of the Matlab toolboxes like the Instrument Control Toolbox (ICT).

The software is structured in several Matlab function files. In the following these functions are explained in more details.

6.2.1 Communication with Equipment

For establishing the communication between the PC and the measurement equipment, the Matlab Instrument Control Toolbox is used. The toolbox supports the most common used communication protocols like GPIB, USB and LAN. Most of the measurement instruments are connected through GPIB cable, because most of the used instruments supports this bus protocol.

Due to a driver failure the oscilloscope cannot be controlled through the GPIB. Therefore, the oscilloscope is connected via an USB cable.

Each measurement instrument is assigned with an unique GPIB address. Listing 6.1 presents the Matlab code, which establish a communication channel to the instruments. The communication is closed at the end of the test procedure.

```
1
2  %% initialize oscilloscope
3  visaObjectOscilloscope = instrfind('Type', 'visa-usb',...
4      'RsrcName', 'USB0::0x0957::0x1744::MY44000305::0::INSTR');
5
6  if isempty(visaObjectOscilloscope)
7      visaObjectOscilloscope = visa('NI',...
8          'USB0::0x0957::0x1744::MY44000305::0::INSTR');
9  else
10     fclose(visaObjectOscilloscope);
11     visaObjectOscilloscope = visaObjectOscilloscope(1)
12 end
13
14 %% initialize smu
15 smu_adcmt_6242 = instrfind('Type', 'gpib', 'BoardIndex', 0,...
16     'PrimaryAddress', 7, 'Tag', '');
17 if isempty(smu_adcmt_6242)
18     smu_adcmt_6242 = gpib('ni', 0, 7);
19 else
20     fclose(smu_adcmt_6242);
21     smu_adcmt_6242 = smu_adcmt_6242(1);
22 end
23
24 %% open communicaton channels
25 fopen(smu_adcmt_6242);
26 fopen(osci_MSO6000);
```

Listing 6.1: Code for establishing the communcation with the instruments.

6.2.2 Data Acquisition

The data is recorded from two measurement instruments; the oscilloscope and the SMU.

Oscilloscope First the oscilloscope has to be configured by setting the input buffer size, the timeout time, the byte-order and the trigger level. The trigger level is set to half of the predefined TLP pulse.

After setup, the oscilloscope remains in waiting mode until it is triggered. Therefore, a while loop is used for polling the trigger event. If this bit is set the polling loop is exited and the measurement tool is halted by a stop command.

During the stopping state it is possible to acquire the measurement data from each channel. The raw data points are downloaded by the command WAV? and they are saved in an unsigned integer16 vector. In order to process the data it is necessary to acquire additional information of the oscilloscope settings by downloading the preamble block information too. All this data is stored in the Matlab struct curvedata. In Table 6.5 the structure of this data is described.

At the end of the channel data acquiring process the oscilloscope is set back to the running mode by sending the command RUN over the bus interface. In Listing 6.2 the Matlab code for getting the oscilloscope data is presented.

```
%Setup Oscilloscope
visaObjectOscilloscope.InputBufferSize = 10000000;
visaObjectOscilloscope.Timeout = 10;
visaObjectOscilloscope.ByteOrder = 'littleEndian';

disp(['triggerEvent:: WAIT FOR TRIGGER - BEGIN']);
while ~isequal(triggerEvent,['+1' char(10)])
    triggerEvent = query(visaObjectOscilloscope,'TER?');
end
disp(['triggerEvent:: WAIT FOR TRIGGER - END']);

% Set Oscilloscope to STOP - MODE
fprintf(visaObjectOscilloscope,':STOP');

% Get data from Channel 1 and Channel 2
curve_data_1 = acquireDataSingleChannel(visaOscilloscope,...
                                                    'CHANNEL1');
curve_data_2 = acquireDataSingleChannel(visaOscilloscope,...
                                                    'CHANNEL2');

% Save Oscilloscope data in TLP Test Data Struct
TLPData.curve_current = curve_data_1;
TLPData.curve_voltage = curve_data_2;

% Set Oscilloscope to RUN - MODE
fprintf(visaObjectOscilloscope,':RUN');
```

Listing 6.2: Code for acquiring the voltage and current curve.

Source Measuring Unit For acquiring the leakage current the SMU is set to current voltage mode. There are two leakage current measurements. The first current is measured while the tested pin of the DUT is set to 0 V. The other current measurement is done while the tested pin is set to 5 V.

After setting the voltage, the leakage is measured and saved in measurement dataset. In Listing 6.3 the Matlab code is shown for getting the leakage current.

Channel Data Entries		
Struct Entry	Type	Additional Notes
dataPoints	Array	the measurement data points
format	int16	0 = byte, 1 = word, 2 = ASCII
type	int16	0 = normal, 1 = peak detect, 2 = average
dataPointsAmount	int32	amount of data points transferred
xFirst	float64	the first data point in memory
yFirst	float32	value is the voltage at center screen
voltsPerDiv	int32	volts per divisions
offset	int32	the offset
secPerDiv	int32	seconds per division
delay	int32	delay time

Table 6.5: Important facts of the oscilloscope take from quote

```
% Trigger mode hold
fprintf(smu_adcmt_6242, 'M1');
% DC mode
fprintf(smu_adcmt_6242, 'MD0');
% Voltage source function
fprintf(smu_adcmt_6242, 'VF');
% source range ? Optimal range
fprintf(smu_adcmt_6242, 'SVRX');
% Sets voltage source value.
fprintf(smu_adcmt_6242, 'SOV0');
% DC current measurement (DCI)
fprintf(smu_adcmt_6242, 'F2');
% output on
fprintf(smu_adcmt_6242, 'OPR');
pause(2);
% trigger
fprintf(smu_adcmt_6242, '*TRG');
% get measurement data from sto1
leakage_current_low = query(smu_adcmt_6242, 'ST1');
% output off
fprintf(smu_adcmt_6242, 'SBY');
```

Listing 6.3: Code for acquiring the leakage current.

6.2.3 Data Processing

This part describes the data format and the Matlab code which is used for generating the I-V curve.

Dataset In Table 6.6 the data structure of the measurement data, which is acquired during a full test loop, is presented. The dataset contains all relevant data of the voltage and current curve at the stressed device pin, the leakage current for 0 V and 5 V and an identifier in order to link the dataset to a specific DUT.

Dataset Description		
Name	Type	Additional Notes
currentCurve	struct	all important information about the voltage curve
voltageCurve	struct	all important information about the current curve
leakageCurrent	int32	leakage current
dutID	int32	id of the DUT

Table 6.6: Structure of the measurement data.

I-V Curve The curve is generated by using the average current and average voltage at the DUT for each stress pulse. The averaged values are plotted against each other. Therefore, the data is saved in a Matlab dataset for further usage.

```
disp('----------TLP Processing Start ---------')
disp('----------TLP Processing Calculating I-V Curve ---------')
for i=1:m
  for i=1:n
    % get data points from dataset
    curve_data_1.X  = measurement_data{i}.curve_channel_1;
    curve_data_2.Y  = measurement_data{i}.curve_channel_2;

    % set range for obtaining data (I/V curve)
    range_start = length(curve_data_1.X) .* 0.3;
    range_end   = length(curve_data_1.X) .* 0.5;

    % calc average
    average_voltage = mean(curve_data_1.Y(range_start:range_end));
    average_current = mean(curve_data_2.Y(range_start:range_end));

    % save avergae values
    iv_data.Icurrent    = average_value_current;
    iv_data.Vvoltage    = average_value_voltage;
    iv_data.current_raw = curve_data_2.YData;
    iv_data.voltage_raw = curve_data_1.YData;
    iv_data.time        = curve_data_1.XData;
    iv_data.settings    = iv_settings;
```

Listing 6.4: Code for generating the I-V curve.

6.2.4 Program Control Flow

At the beginning of each test session the TLP generator is configured with the parameters pulse voltage and pulse width.

Next, the range for the oscilloscope is set. It is assumed that the DUT voltage is half the settings of the TLP generator voltage. For the current measurements it is very difficult to estimate the current curve, since it is not known which protection circuit the DUT uses.

After the range setup is done the test and measurement equipment is ready for the test and the TLP is fired to the device. The current and voltage curve is captured by the oscilloscope. If data points are out of the oscilloscope range, the scale parameter of the instrument is increased by user defined

value. The new range settings will be used and the DUT will be stressed again with the same TLP voltage until the data is in range.

Only when the measurement data is in range the leakage current will be measured. After the leakage current measurement the TLP voltage will be incremented and the test procedure will start again. Figure 6.2 shows the implemented test algorithm.

Due to the fact that a suitable automated test handler is not available, it is necessary to change the DUT after the end of the test process manually.

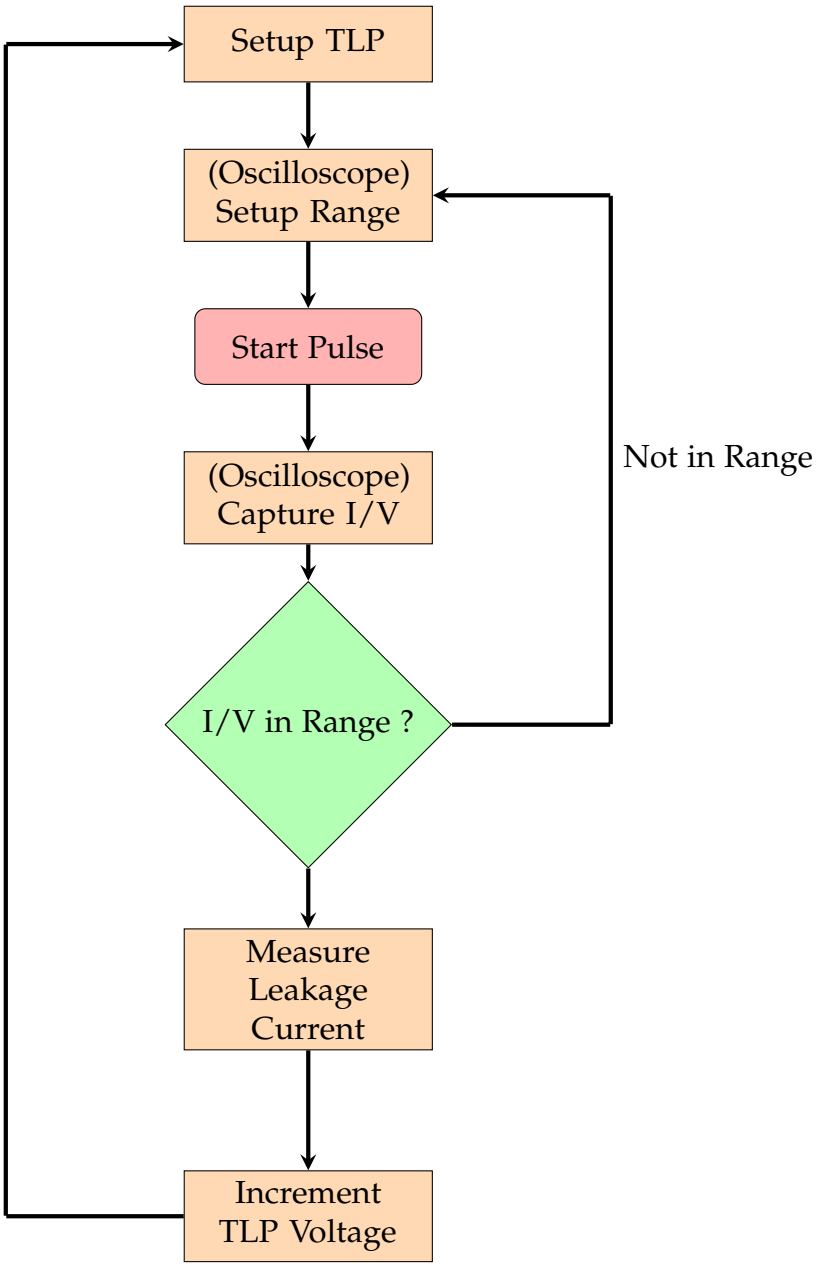

Figure 6.2: Program control flow of the TLP testing.

7 TLP Test Results

Within this thesis, a RS-485 transceiver chip (SP485R) is investigated. The internal protection structure of the transceiver is unknown. The transceiver is tested using the setup described in Section 6.1.1. Pin A is the pin under test. All other pins are connected to ground. The measurement results are presented in this chapter to evaluate the functionality of the test setup and software.

During the measurement the TLP pulse width is set to 100 ns. The TLP voltage is varied from 30 V to 130 V in steps of 10 V. For each pulse the oscilloscope records the current through and the voltage at the device, as illustrated in Figure 7.1a and Figure 7.1b, respectively.

Figure 7.1a shows the recorded voltage curve at the DUT for a TLP voltage of 100 V. At the beginning, a transient peak can be observed, then the voltage settles to constant value. The individual data points still change over time in this regime. In order to assign a voltage value to the TLP voltage, the data points from the last third of the pulse are averaged. At the end of the pulse, the voltage at the device becomes 0 V again.

The same data processing is applied to the current data through the DUT. Figure 7.1b presents the recorded current curve. In contrast to the voltage curve, no transient peak at the beginning can be observed. Again, the data points from the last third are averaged.

This procedure is applied to all pulses and the averaged voltages are plotted against the averaged current values. Figure 7.2 shows the resulting I-V curve.

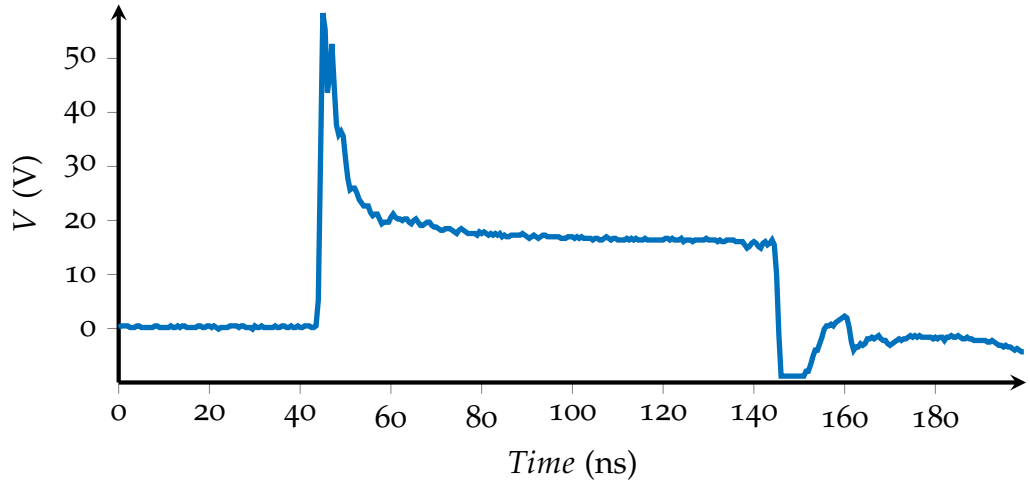

(a)

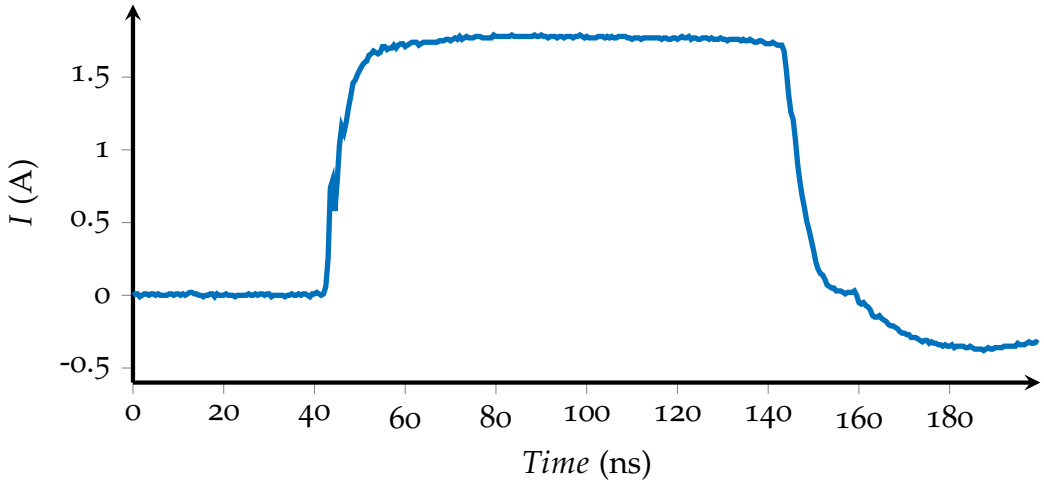

(b)

Figure 7.1: Measurement results for a 100 ns TL pulse of 130V, recorded with an oscilloscope. (a) shows the voltage at the device and (b) current through the device.

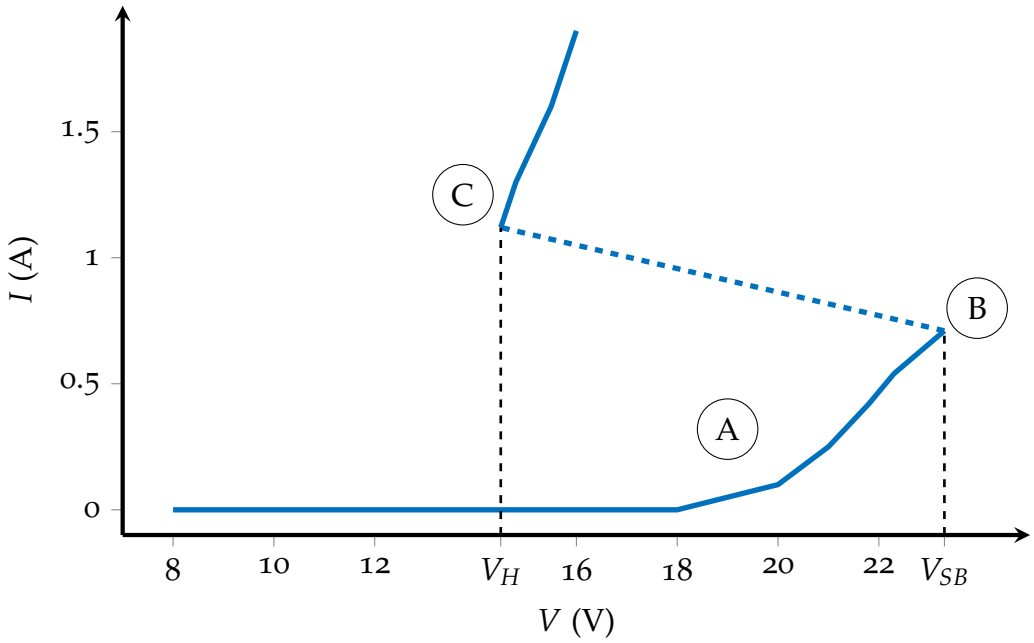

Figure 7.2: Snap-back characteristic of the DUT for a TL pulse of 100 ns. (A) marks the on-set of current flow. (B) marks the snap-back point. (C) marks the holding point.

- **A**: Increasing the TLP voltage first yields an increase of the voltage at DUT. After a certain voltage is reached, also a current starts to flow through the DUT.
- **B**: When a certain pulse amplitude is exceeded, the protection structure is activated and it diverts a part of the current. The device voltage at this pulse height is denoted snap-back voltage V_{SB}
- **C**: The voltage at the device falls back to the so-called holding voltage V_H. Further increasing the pulse height again results in an increase of the voltage at the device beyond V_H.

8 Conclusions and Outlook

In the course of this thesis, a concept for an automated TLP test system has been developed. The automation is based on a gravity test handler, which places the electronic devices on the test board.

The test handler was available and put into operation. Unfortunately, its application was limited to a specific chip package type and its maintenance and operation would have been too time-consuming. Therefore, the test handler was finally set aside and the chips were placed manually.

A RS-485 transceiver chip, with an unknown internal protection structure, was tested with TLP. From the measured current and voltage curves for different pulse amplitude it was concluded, that the chip features a snap-back protection structure.

One key aspect of this thesis was the design and implementation of test and measurement software, especially the software for controlling the test equipment, capturing the measurement data and the further data processing. It is now possible to record I-V curves in a very short time.

In order to record Wunsch-Bell characteristics in a reasonable time, an automated test handler, which supports a variety of package types, is strongly suggested. Due to the lack of time, the Wunsch-Bell characteristics were not generated. Another improvement would be the using a remote-controllable TLP generator.

Bibliography

[1] H. A. Gieser and H. Wolf, "Survey on Very Fast TLP and Ultra Fast Repetitive Pulsing for Characterization in the CDM-Domain," in *Reliability Physics Symposium, 2007. Proceedings. 45th annual. IEEE International*, IEEE, 2007, pp. 324–333 (cit. on p. 3).

[2] A. Amerasekera, E. A. Amerasekera, and D. Charvaka, *ESD in Silicon Integrated Circuits*. John Wiley & Sons, 2002 (cit. on pp. 3, 7, 29–32).

[3] K. L. Kaiser, *Electrostatic Discharge*. CRC PR INC, 2005 (cit. on p. 4).

[4] P. A. Tipler and G. Mosca, *Physik: Für Wissenschaftler und Ingenieure*, Zweite Edition. Springer-Verlag, 2004 (cit. on p. 6).

[5] J. Vinson and J. Liou, "Electrostatic Discharge in Semiconductor Devices: An Overview," *Proceedings of the IEEE*, vol. 86, no. 2, pp. 399–420, 1998 (cit. on pp. 7, 11).

[6] W. Simbürger, *Effective ESD Protection Design at System Level using VF-TLP Characterization Methodology*, Infineon Application Note 210, Dec. 2012 (cit. on p. 7).

[7] S. H. Voldman, *Electrical Overstress (EOS): Devices, Circuits and Systems*. John Wiley & Sons, 2013 (cit. on pp. 9, 17).

[8] D. Pierce and D. Durgin, "An Overview of Electrical Overstress Effects on Semiconductor Devices," in *Proceedings of the EOS/ESD Symposium*, 1981, p. 120 (cit. on pp. 11, 14).

[9] N. Azizi and P. Yiannacouras, "Gate Oxide Breakdown," *Lecture Notes, Reliability of Intergrated Circuits*, 2003 (cit. on p. 11).

[10] S. Ben Dhia, M. Ramdani, and E. Sicard, *Electromagnetic Compatibility of Integrated Circuits*. Springer-Verlag GmbH, 2005 (cit. on pp. 16–23).

[11] J. Vinson and J. Liou, "Electrostatic Discharge in Semiconductor Devices: Overview of Circuit Protection Techniques," in *Electron Devices Meeting, 2000. Proceedings. 2000 IEEE Hong Kong*, 2000, pp. 5–8 (cit. on pp. 20, 22).

[12] F. zur Nieden, B. Arndt, J. Edenhofer, and S. Frei, "Vergleich von ESD-System-Level Testmethoden für Packaging und Handling," *ESD FORUM, Berlin*, 2009 (cit. on p. 22).

[13] ThermoFisher Scientific, *Introduction to Transmission Line Pulse*, Presentation Slides, Feb. 2016 (cit. on p. 22).

[14] T. Maloney and N. Khurana, "Transmission Line Pulsing Techniques for Circuit Modeling of ESD Phenomena," in *Proc. EOS/ESD Symposium*, vol. 7, 1985, pp. 49–54 (cit. on p. 22).

[15] W. Simbürger, D. Johnsson, and M. Stecher, "High Current TLP Characterisation: An Effective Tool for the Development of Semiconductor Devices and ESD Protection Solutions," *ARMMS RF & Microwave Society*, 2012 (cit. on pp. 23, 26).

[16] D. Wunsch and R. Bell, "Determination of Threshold Failure Levels of Semiconductor Diodes and Transistors due to Pulse Voltages," *IEEE Transactions on Nuclear Science*, vol. 15, no. 6, pp. 244–259, 1968 (cit. on p. 27).

[17] S. H. Voldman, *ESD: Physics and Devices*. John Wiley & Sons, 2004 (cit. on p. 27).

[18] S. G. Beebe, "Characterization, Modeling, and Design of ESD Protection Circuits," PhD thesis, Stanford, 1998 (cit. on p. 27).

[19] K. B. Schaub and J. Kelly, *Production Testing of RF and System-on-a-chip Devices for Wireless Communications*. Artech House, 2004 (cit. on p. 33).

[20] USB Implementers Forum, *Universal Serial Bus Specification* (cit. on p. 36).

[21] I. Electronics, *Gpib 101 - a tutorial about the gbip bus* (cit. on p. 36).

[22] National Intruments, *Installation Guide GPIB-USB-HS* (cit. on p. 36).

[23] ADCMT, *6241A/6242 DC Voltage Current Source/Monitor Operation Manual* (cit. on p. 41).